Implementation and Validation of a Docking System for Nonholonomical Vehicles

João Barbosa[1], Carlos Cardeira[1], and Paulo Oliveira[1,2]

[1] IDMEC/LAETA - Instituto Superior Técnico, Universidade de Lisboa, 1049-001 Lisboa, Portugal
[2] ISR - Instituto Superior Técnico Universidade de Lisboa, 1049-001 Lisboa, Portugal

Abstract. This paper presents the experimental validation of a docking system for a differential drive robot. The docking problem is solved with a smooth, time-invariant, globally asymptotically stable feedback control law which allows for a very human-like closed-loop steering that drives the robot to a certain goal with a desired attitude and a tunable curvature. Simulations of the docking problem are presented that illustrate the performance of the system and it is also validated by performing tests on the aforementioned real robot.

Keywords: Docking, Mobile Robots, Nonlinear Control, Lyapunov Techniques.

1 Introduction

Industrial automation has experienced huge advance in the last decades [1]. Flexible automation manufacturing cells require the use of automatic handling solutions usually resorting to Automatic Guided Vehicles (AGVs). Nowadays the fleets of AGVs must navigate among warehouses, automated workcells, and charging stations. Thus, the automated docking of mobile robotic platforms, such as AGVs, with minimal structuring of the environment is still a active topic of research [2]. The solutions found in the literature to solve this problem vary both in algorithm and sensor payload. One approach, defined as visual servoing, with an early contribution reported in [3], consists of representing a given task directly by an error relative to a goal image to be captured by the vision system. This approach became popular from 1990 onward with works such as [4], with a great contribute of the task function approach [5]. Visual servoing benefits from contributes with out-of-body cameras, i.e., Camera-Space Manipulation (CSM) [6], Mobile Camera-Space Manipulation (MCSM) which extends the latter with body embedded cameras and, more recently, [7] which computes the goal configuration using visual landmarks. Other approaches to the docking problem include the computation of feedback control laws by using Lyapunov and backstepping techniques that lead to an Ultra-Short Baseline (USBL) acoustic positioning system [8] applied on the underwater counterpart of this work, the use of electromagnetic homing systems [9], optical guidance approaches such as [10] and computing the deceleration needed by a robot,

A.P. Moreira et al. (eds.), *CONTROLO'2014 - Proc. of the 11th Port. Conf. on Autom. Control*, Lecture Notes in Electrical Engineering 321, DOI: 10.1007/978-3-319-10380-8_50

resorting to an estimation of a *time-to-contact* (τ) through optical flow field divergence measurements of an image stream as in [11] and references therein. In [12] a method based on the direction of arrival (DOA) of signals transmitted by RFID transponders is proposed, showing that a robot can dock in a station transmitting through an RFID by using two antennae installed on-board of the vehicle. A method proposing the estimation of the position and orientation of a visual landmark is presented in [13] to help on docking and automatic recharging, thus being similar to the work presented herein.

This work validates a functional docking system using a full state feedback law inspired in [14] which drives a nonholonomic vehicle from any initial position to a certain defined goal with a desired attitude. Mobile robots resorting to vision systems allow for more versatility in an industrial facility regarding docking stations, positioning of cargo pallets, consequently simplifying the overall task of map building and task planning, dropping the need of extreme precision regarding these actions.

The present paper is organised as follows: Details on the feedback control law used in this work are presented in Section 2, which is followed by the results of real-time experiments in Section 3. Finally, some conclusions on the overall performance of the proposed strategies are drawn in Section 4.

2 Docking Problem

In this section, the model of the mobile robot and the operation environment is introduced (see [15] for details) and the implemented control law is described. Suppose the state of the robot is $\mathbf{z} = [e_x\ e_y\ \psi]^T \in \mathcal{R}^3$ composed by quantities depicted in Fig. 1. Representing the docking station position $\mathbf{e}(t) \in \mathcal{R}^2$ and attitude $\psi(t) \in \mathcal{R}$ in the body frame allows for the derivation of linear kinematics and output equations. Furthermore, it is also possible to estimate linear and angular slippages, respectively $b \in \mathcal{R}$ and $s \in \mathcal{R}$, that may occur due to the lack of knowledge of the contact points with the floor as well as the lack of precision in the measurement of each wheel radius or asymmetries in mechanical construction. Both slippages are considered to be slow time-varying or even constant ($\dot{b} = 0$ and $\dot{s} = 0$). The state vectors estimated by the position and attitude estimators are, respectively, $\mathbf{x} = \begin{bmatrix}\mathbf{e}^T & b\end{bmatrix}^T$ and $\boldsymbol{\theta} = [\psi \quad s]^T$. Both systems are represented in (1)

$$\begin{cases}\dot{\boldsymbol{\theta}}(t) = \mathbf{A}^{\boldsymbol{\theta}}\boldsymbol{\theta}(t) + \mathbf{B}^{\boldsymbol{\theta}}\omega(t) + \boldsymbol{\nu}(t) \\ y(t) = \psi(t) + \eta(t)\end{cases}, \tag{1}$$

where

$$\mathbf{A}^{\boldsymbol{\theta}} = \begin{bmatrix}0 & -1 \\ 0 & 0\end{bmatrix}, \mathbf{B}^{\boldsymbol{\theta}} = \begin{bmatrix}-1 \\ 0\end{bmatrix},$$

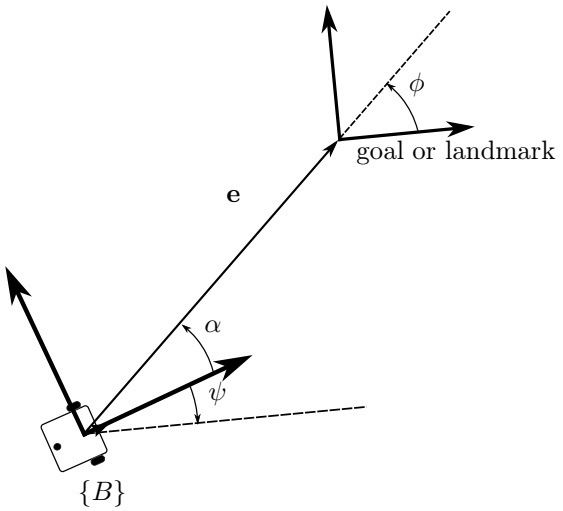

Fig. 1. Depiction of robot and docking station frames

and (2)

$$\begin{cases} \dot{\mathbf{x}}(t) = \mathbf{A}^{\mathbf{x}}(\omega(t))\mathbf{x}(t) + \mathbf{B}^{\mathbf{x}}\bar{v}(t) + \mathbf{v}(t) \\ \mathbf{y}(t) = \mathbf{e}(t) + \mathbf{w}(t) \end{cases}, \tag{2}$$

where

$$\mathbf{A}^{\mathbf{x}}(\omega(t)) = \begin{bmatrix} 0 & \omega & -1 \\ -\omega & 0 & 0 \\ 0 & 0 & 0 \end{bmatrix}, \mathbf{B}^{\mathbf{x}} = \begin{bmatrix} -1 \\ 0 \\ 0 \end{bmatrix}.$$

Notice that both systems are linear and do not make use of any approximation. Furthermore, (1) originates an optimal observer and (2) a sub-optimal one, as ω is a measured quantity, rather than a known one. Both systems are proven observable and their Kalman Filter application is detailed in [15].

Notice now that $\mathbf{z} = [e_x\ e_y\ \psi]^T$ can be represented in the form

$$\dot{\mathbf{z}} = \mathbf{f}_\omega(\mathbf{z})\omega + \mathbf{f}_v(\mathbf{z})v, \tag{3}$$

where

$$\mathbf{f}_\omega = \begin{bmatrix} e_y \\ -e_x \\ -1 \end{bmatrix}, \quad \mathbf{f}_v = \begin{bmatrix} -1 \\ 0 \\ 0 \end{bmatrix}.$$

The present work follows Lyapunov's direct method of finding a scalar energy-like function $V(\mathbf{z})$ and devise a control law $\mathbf{u}(\mathbf{z})$ that ensures the resulting closed-loop system is asymptotically stable (the goal is to park the vehicle in a position $\mathbf{z}^*$). This leads to a smooth and time invariant control law. However, a theorem developed by Brockett shown in [16], states that, for systems in the structure

$$\dot{\mathbf{z}} = \sum_{i=1}^{m} \mathbf{f}_i(\mathbf{z}) u_i,$$

with vectors $\mathbf{f}_i(\mathbf{z})$ being linearly independent and continuously differentiable at a point z^*, then there exists a stabilization solution, with a smooth and time invariant feedback law, if and only if $m = n$, where n is the order of the system, meaning there need to be the same number of control parameters as the dimension of the state vector to be controlled. The system in (3) does not respect the last condition and clearly has $\mathbf{f}_\omega$ and $\mathbf{f}_v$ independent at the origin. This would then require the use of time-varying or discontinuous control laws in order to achieve the desired stabilization. Seeing as the need of stabilizing n states at a point $\mathbf{z}^*$ is still the objective, then only a system with singularities is of interest. With this in mind, a new system is proposed in [14]. The said system, represented in (4), is based on a state vector that is isomorphic with the one in (3), characterized by the isomorphism $g : \mathbb{R}^3 \setminus \{\mathbf{0}\} \mapsto \mathbb{R}^3 \setminus \{\mathbf{0}\}$

$$\begin{cases} e = \|\mathbf{e}\| \\ \alpha = atan(e_y/e_x) \\ \phi = atan(e_y/e_x) - \psi \end{cases},$$

variables depicted in Figure 1, leading to the kinematics

$$\begin{cases} \dot{e} = -v\cos\alpha \\ \dot{\alpha} = -\omega + v\frac{\sin\alpha}{e} \\ \dot{\phi} = v\frac{\sin\alpha}{e} \end{cases}. \tag{4}$$

Due to the singularity at the origin, Brockett's theorem no longer applies, since the regularity assumptions do not hold, and so the asymptotic stabilization of (4) is possible. One then cannot formally use the definition of equilibrium point to describe the origin, since it is now located in the frontier of the open set of validity of the system dynamics. The objective of the control law is then to asymptotically drive the system to ${\mathbf{z_p}}^* = [0 \quad 0 \quad 0]^T$ without attaining $e = 0$ in a finite time, where $\mathbf{z_p} = [e \quad \alpha \quad \phi]$ is henceforth the notation used for the new state vector. A simple choice for a candidate Lyapunov function is the often used quadratic error form

$$V(\mathbf{z}) = \underbrace{\frac{1}{2}\lambda e^2}_{V_1} + \underbrace{\frac{1}{2}\alpha^2 + \frac{1}{2}h\phi^2}_{V_2}, \quad \lambda, h > 0 \tag{5}$$

where λ and h are positive weighting constants that will help shape the control law. By separating the scalar function in two terms, we have that the first term refers to the error in distance to the target position, and the second term corresponds to the to a "alignment vector" error $\begin{bmatrix}\alpha & \sqrt{h}\phi\end{bmatrix}$. It is clear by now that the a candidate of a scalar function has been chosen and then a function $\mathbf{u}(\mathbf{z_p})$ will be derived in order for the behaviour of V along the trajectory of (4) to drive the state asymptotically to the origin. Taking then the derivative $\dot{V}$, given by

$$\begin{aligned}\dot{V} &= \lambda e\dot{e} + \left(\alpha\dot{\alpha} + h\phi\dot{\phi}\right) \\ &= \lambda ev\cos\alpha + \alpha\left[-\omega + v\frac{\sin\alpha(\alpha + h\phi)}{\alpha e}\right].\end{aligned} \tag{6}$$

The first term of (6) can be made non-positive by letting

$$v = \gamma e\cos\alpha, \quad \gamma > 0, \tag{7}$$

leading to

$$\dot{V}_1 = -\lambda\gamma\cos^2\alpha e^2 \leq 0. \tag{8}$$

This choice of linear velocity control law ensures that the validity of (4) throughout the parking problem, since V_1 is lower bounded and non-increasing, making it asymptotically converge to a non negative finite limit, thus ensuring e exhibits the same behaviour. The same strategy is applied to the second term, and so expression for the angular velocity control law is

$$\begin{aligned}\omega &= k\alpha + v\frac{\sin\alpha(\alpha + h\phi)}{\alpha e} \\ &\overset{(7)}{=} k\alpha + \gamma\frac{\cos\alpha\sin\alpha(\alpha + h\phi)}{\alpha}.\end{aligned} \tag{9}$$

The derivative of the total Lyapunov function then becomes

$$\dot{V} = -\gamma\left(\cos^2\alpha\right)e^2 - k\alpha^2 \leq 0, \tag{10}$$

which is negative semi definite. It is however possible, as described in [14], to prove that the origin is globally asymptotically stable by using LaSalle's theorem and Barbalat's Lemma upon the inspection of the resulting closed-loop system. Note that the objective is to have the vehicle dock in a certain station with positive linear velocity, but it is possible to obtain different trajectories by simply changing the goal objective (to for instance $\mathbf{z_p}^* = [0, \pm\pi, \pm\pi]$). A depiction of the trajectories performed by the system are depicted in Fig. 2, where a simulation was performed with $\gamma = 3$, $h = 1$ and $k = 6$.

As intended, the vehicle always arrives at the target location facing, which goes accordingly with state vector converging to the origin.

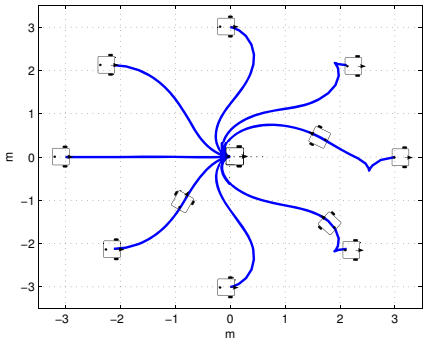

Fig. 2. Trajectories performed with $e(0) = 3$ and $\psi(0) = 0$

3 Experimental Results

The focus of this section is the validation of the docking solution. The robot prototype and landmark setup are shown in Fig. 3. The architecture of the localization system that provides the necessary measurements is represented in Fig. 4. Below is a summary of the parameters and initialization of both Kalman Filters used in the observer.

- Camera noise covariance: $\mathbf{R}^{\mathbf{x}} = 1 \times 10^{-2}\mathbf{I}_2$ and $\mathbf{R}^{\theta} = 1 \times 10^{-2}$
- Plant noise covariance: $\mathbf{Q}^{\mathbf{x}} = diag(4.1 \times 10^{-6}\mathbf{I}_2, 1 \times 10^{-8})$ and $\mathbf{Q}^{\theta} = diag(2 \times 10^{-5}, 1 \times 10^{-8})$
- Initial covariance matrix: $\mathbf{P}_0^{\mathbf{x}} = 1\mathbf{I}_3$ and $\mathbf{P}_0^{\theta} = 0.1\mathbf{I}_3$
- Initial conditions: $\hat{\mathbf{e}}$ and $\hat{\theta}$ were set to the real initial position, and both bias estimates $\hat{b}$ and $\hat{s}$ were set to zero.

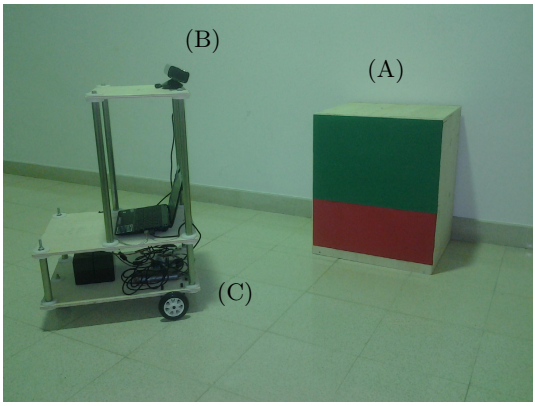

Fig. 3. (A) Docking station, (B) 3D camera and (C) Robot prototype

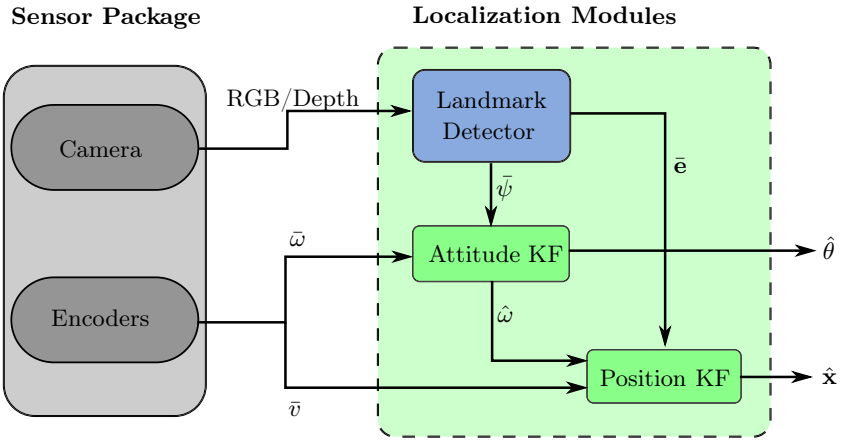

Fig. 4. Estimator Modules

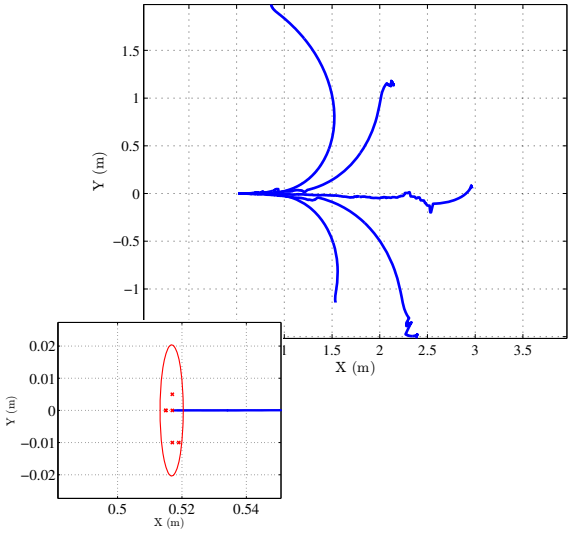

Fig. 5. Depiction of several docking manoeuvres and their 3σ error confidence and ground truth of the final position (zoom)

Table 1. Error in docking manoeuvres

	μ	σ
$e_x\ [cm]$	3.5	0.12
$e_y\ [cm]$	−0.5	0.61
$\psi\ [°]$	0.08	0.285

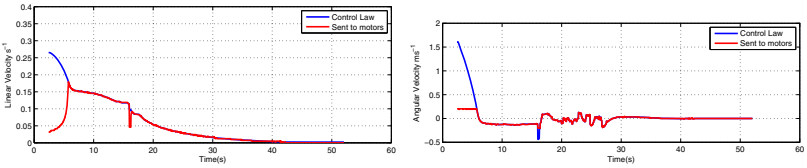

(a) Linear velocity command (b) Angular velocity command

Fig. 6. Time progression of commands

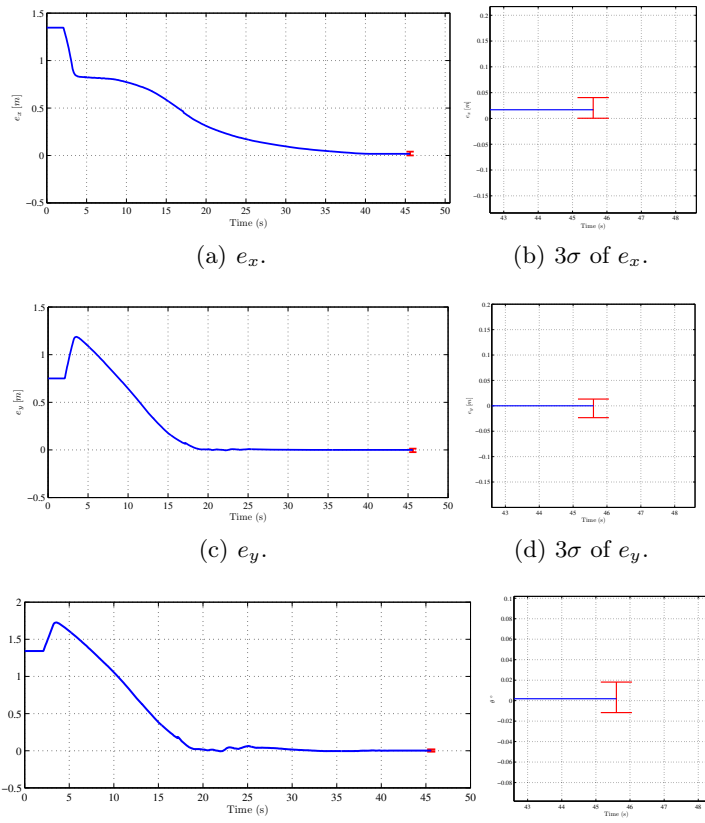

(a) e_x. (b) 3σ of e_x.

(c) e_y. (d) 3σ of e_y.

(e) θ. (f) 3σ of θ.

Fig. 7. Time progression of state variables and the 3σ interval for final position

For the tests presented in this section, the landmark or docking station is considered to be the origin of the inertial frame and the goal of every experiment presented in this section was set $0.5\,m$ in front of the real landmark object being used. Also, in every experiment, unless stated otherwise, the initial estimate of the position was very near the real position of the mobile robot, seeing as the

estimation filters were active before the feedback loop was enabled. A saturation of $v_{max} = 0.2\, ms^{-1}$ and $\omega_{max} = 0.2\, ms^{-1}$. Figure 5 depicts the localisation estimate and true final position of several tests carried out in the laboratory environment. In each one of the 6 tests, represented in zoom of Fig. 5, the prototype was able to perform a successful docking manoeuvre, even when the initial estimate had a slight error. The final position error is represented in Table 1.

In Fig. 6 the commands in a particular experiment are shown and the effect that the correction of the estimate in them while Fig. 7 depicts the state variables converging to zero. Notice that, due to the discrete nature of commands, the vehicle never reaches the goal completely, and the error distance to the target will depend on the value of γ and the error in the camera to body transposition and rotation calibrations.

4 Conclusions and Further Work

The implemented feedback control successfully drives the robot to a given goal and is tunable to the needs of the localisation system, seeing as it is possible to require the robot to take the same path under different speeds by just adjusting the parameters that tune the feedback. It is also possible to achieve good results by imposing a saturation in linear and angular velocities as to ensure convergence of the localisation system within the manoeuvre time frame. The robot is able to drive itself to the correct goal even when a wrong initial position and attitude estimate occurs, given that the docking station is, at some point, visible by the sensor package. The error of the docking manoeuvre, within 3σ tolerance, is $3\sigma_x = 0.36\, cm$, $3\sigma_y = 1.83\, cm$ and $3\sigma_\theta = 0.855\,^\circ$, being that most of it was due to uncertainties in the camera transform and due to the quantization of the motor commands. Also note that the 3D camera does not recognize the docking station upon the final approach segment of the manoeuvres, which corresponds to a $1\, m$ distance, resulting in odometry navigation during the last part of each docking. The accuracy may improve in further work which includes other sensors with better accuracy, such as laser range-finders, to avoid the odometry errors during the last segment. This work can go towards 3D manoeuvres (with other vehicles and models) and cooperative manoeuvres among multiple robots.

Acknowledgements. This work was supported by FCT, through IDMEC, under LAETA Pest-OE / EME / LA0022 and partially supported by the project PRODUTECH-PTI (Proj. 3904) under the program COMPETE / QREN / FEDER.

References

1. Groover, M.P.: Automation, Production Systems, and Computer-Integrated Manufacturing, 3rd edn. Prentice Hall Press, Upper Saddle River (2007)

2. Hada, Y., Yuta, S.: A first-stage experiment of long term activity of autonomous mobile robot result of repetitive base-docking over a week. In: Rus, D., Singh, S. (eds.) Experimental Robotics VII. LNCIS, vol. 271, pp. 229–238. Springer, Heidelberg (2001)
3. Agin, G.J.: Real time control of a robot with a mobile camera. SRI International (1979)
4. Espiau, B., Chaumette, F., Rives, P.: A new approach to visual servoing in robotics. IEEE Transactions on Robotics and Automation 8(3), 313–326 (1992)
5. Samson, C., Espiau, B., Borgne, M.L.: Robot control: the task function approach. Oxford University Press (1991)
6. Skaar, S.B., Yalda-Mooshabad, I., Brockman, W.H.: Nonholonomic camera-space manipulation. IEEE Transactions on Robotics and Automation 8(4), 464–479 (1992)
7. Lefebvre, O., Lamiraux, F.: Docking task for nonholonomic mobile robots. In: Proceedings of the 2006 IEEE International Conference on Robotics and Automation, ICRA 2006, pp. 3736–3741. IEEE (2006)
8. Batista, P., Silvestre, C., Oliveira, P.: A two-step control strategy for docking of autonomous underwater vehicles. In: American Control Conference (ACC), pp. 5395–5400. IEEE (2012)
9. Feezor, M.D., Yates Sorrell, F., Blankinship, P.R., Bellingham, J.G.: Autonomous underwater vehicle homing/docking via electromagnetic guidance. IEEE Journal of Oceanic Engineering 26(4), 515–521 (2001)
10. Park, J.Y., Jun, B.H., Lee, P.M., Lee, F.Y., Oh, J.H.: Experiment on underwater docking of an autonomous underwater vehicleisimi'using optical terminal guidance. In: OCEANS 2007-Europe, pp. 1–6. IEEE (2007)
11. McCarthy, C., Barnes, N., Mahony, R.: A robust docking strategy for a mobile robot using flow field divergence. IEEE Transactions on Robotics 24(4), 832–842 (2008)
12. Kim, M., Chong, N.Y.: Direction sensing rfid reader for mobile robot navigation. IEEE Transactions on Automation Science and Engineering 6(1), 44–54 (2009)
13. Luo, R.C., Liao, C.T., Su, K.L., Lin, K.C.: Automatic docking and recharging system for autonomous security robot. In: 2005 IEEE/RSJ International Conference on Intelligent Robots and Systems (IROS 2005), pp. 2953–2958. IEEE (2005)
14. Aicardi, M., Casalino, G., Bicchi, A., Balestrino, A.: Closed loop steering of unicycle like vehicles via lyapunov techniques. IEEE Robotics & Automation Magazine 2(1), 27–35 (1995)
15. Barbosa, J.: Design and Validation of a Docking System for Nonholonomical Vehicles. Master's thesis, Instituto Superior Técnico, Universidade de Lisboa (2014)
16. Brockett, R.W., et al.: Asymptotic stability and feedback stabilization. In: Differential Geometric Control Theory, pp. 181–191. Defense Technical Information Center (1983)